

Synthesis and Characterization of Cross-Linked Reverse Micelles

Hyun M. Jung, Kristin E. Price, and D. Tyler McQuade*

Contribution from the Department of Chemistry and Chemical Biology, Cornell University, Ithaca, New York 14853-1301

Received June 6, 2002; E-mail: dtm25@cornell.edu

Abstract: The design and synthesis of a new cross-linkable amphiphile is reported. Solutions of the amphiphile in a toluene/water mixture form reverse micelles as indicated by dynamic light scattering and NMR spectroscopy. As indicated by dynamic light scattering, TEM, and NMR spectroscopy data, these reverse micelles can be cross-linked without drastically changing the radius of the reverse micelles. Mixed reverse micelles are also characterized and cross-linked. The cross-linked reverse micelles are demonstrated to facilitate phase transfer and can be used to site isolate a catalyst.

Introduction

Both small molecule and macromolecular amphiphiles can self-assemble into a wide array of soluble organized structures,¹ including micellar, cylindrical micellar, vesicular, and lamellar phases as well as phases that tend to be insoluble, including hexagonal and bicontinuous phases. These organized materials have been used in a wide variety of applications including detergents,² paints,³ drug delivery agents,⁴ photonic materials,⁵ and scaffolds for creating ordered inorganic materials.⁶

Because these materials are self-assembled, they undergo phase transitions as a function of percent composition and temperature. Capturing the mesophase structure requires covalent linking. Many phases have been captured via polymerization or cross-linking: micelles,⁷ reverse micelles (RMs),⁸ cylindrical micelles,⁹ vesicles,¹⁰ monolayers,¹¹ hexagonal phases,¹² and bicontinuous phases.¹³ The extent to which a lyotropic phase is

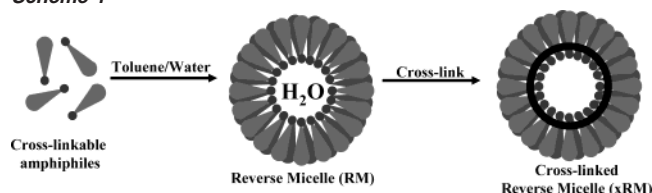
captured depends on the dynamics of the assembly. For example, micelles¹⁴ and RMs composed of small molecules have been polymerized, resulting in molecular weights that are orders of magnitude higher than the weight of the prepolymerized object. Specifically, in the case of RMs, polymerization results in the formation of particles that are roughly 20 times larger than the prepolymerized aggregates.¹⁵ *In other words, RMs have not been captured to provide nanometer size domains,* Scheme 1.

Inverse phases such as RMs and inverse hexagonal phases are unique because they place high functional group density toward a core or narrow channel, respectively, and this density can provide unique reactivity.¹⁶ RMs are spherical entities made by dissolving an amphiphile in an oil/water mixture. Under these conditions, the polar headgroup of the amphiphile partitions at the oil–water interface, creating a water core that is typically 10–100 Å in diameter.¹⁷ The small spherical nature of RMs allows facile movement of materials in and out of the core. Functional group density around the core and permeability make RMs particularly attractive candidates for microreactors.¹⁸ One limitation of RMs is their capacity to undergo facile phase transitions, thereby limiting the temperature range in which they can be used. Before the range of RM microreactor applications can be realized, a methodology enabling covalent capture that retains the prepolymerized morphology of the RMs must be

- (1) (a) For a review of block copolymer assembly, see: Klok, H.-A.; Lecommandoux, L. *Adv. Mater.* **2001**, *13*, 1217. (b) For surfactant phase behavior in aqueous solutions, see: Laughlin, R. G. *The Aqueous Phase Behavior of Surfactants*; Academic Press: New York, 1994. (c) For surfactants phase behavior in oil/water mixtures, see: *Reverse Micelles: Biological and Technological Relevance of Amphiphilic Structures in Apolar Media*; Luisi, P. L., Struab, B. E., Eds.; Plenum Press: New York, 1982.
- (2) Lele, B. S.; Leroux, J. C. *Macromolecules* **2002**, *35*, 6714.
- (3) Baradie, B.; Shoichet, M. S. *Macromolecules* **2002**, *35*, 3569.
- (4) (a) Discher, D. E.; Eisenberg, A. *Science* **2002**, *297*, 967. (b) Liu, J. Q.; Zhang, Q.; Remsen, E. E.; Wooley, K. L. *Biomacromolecules* **2002**, *3*, 362.
- (5) Edrington, A. C.; Urbas, A. M.; DeRege, P.; Chen, C.; Swager, T. M.; Hadjichristidis, M.; Xeridou, M.; Fetters, L. J.; Joannopoulos, J. D.; Fink, Y.; Thomas, E. L. *Adv. Mater.* **2001**, *13*, 421.
- (6) Schuth, F. *Chem. Mater.* **2001**, *13*, 3184.
- (7) Qi, Z.; Remsen, E. E.; Wooley, K. L. *J. Am. Chem. Soc.* **2000**, *122*, 3642.
- (8) (a) Voortmans, G.; Verbeeck, A.; Jackers, C.; De Schryver, F. C. *Macromolecules* **1988**, *21*, 1977. (b) Nagai, K.; Satoh, H.; Noriyuki, K. *Polymer* **1993**, *34*, 4969.
- (9) For an excellent investigation of structure evolution during micelle polymerization, see: Kline, S. J. *J. Appl. Crystallogr.* **2000**, *33*, 618.
- (10) (a) Fendler, J. H. *Science* **1984**, *223*, 878. (b) Discher, D. E.; Eisenberg, A. *Science* **2002**, *297*, 967. (c) Mueller, A.; O'Brien, D. F. *Chem. Rev.* **2002**, *102*, 727.
- (11) See: Alekseev, A. S.; Viitala, T.; Domnin, I. N.; Koshkina, I. M.; Nikitenko, A. A.; Peltonen, J. *Langmuir* **2000**, *16*, 3337 and reference therein.
- (12) (a) Hai, D.; Gin, D. L.; Smith, R. C. *J. Am. Chem. Soc.* **1998**, *120*, 3522. (b) Miller, S.; Ding, J. H.; Gin, D. L. *Curr. Opin. Colloid Interface Sci.* **1999**, *4*, 338.

- (13) Hentze, H.-P.; Antonietti, M. *Curr. Opin. Solid State Mater. Sci.* **2001**, *5*, 343.
- (14) Cochin, D.; Zana, R.; Candau, F. *Macromolecules* **1993**, *26*, 5765.
- (15) Voortmans, G.; Verbeeck, A.; Jackers, C.; De Schryver, F. C. *Macromolecules* **1988**, *21*, 1977.
- (16) Gin, D. L.; Gu, W. Q.; Pindzola, B. A.; Zhou, W. J. *Acc. Chem. Res.* **2001**, *34*, 973.
- (17) Moulik, S. P.; Paul, B. K. *Adv. Colloid Interface Sci.* **1998**, *78*, 99.
- (18) (a) Silber, J. J.; Biasutti, A.; Abuin, E.; Lissi, E. *Adv. Colloid Interface Sci.* **1999**, *82*, 189. (b) Correa, N. M.; Durantini, E. N.; Silber, J. J. *J. Org. Chem.* **1999**, *64*, 5757. (c) Van Vyve, F.; Renkin, A. *Catal. Today* **1999**, *48*, 273. (d) Correa, N. M.; Durantini, E. N.; Silber, J. J. *J. Org. Chem.* **2000**, *65*, 6427. (e) Garcia-Rio, L.; Leis, J. R.; Moreira, J. A. *J. Am. Chem. Soc.* **2000**, *122*, 10325. (f) Manabe, K.; Mori, Y.; Wakabayashi, T.; Nagayama, S.; Kobayasi, S. *J. Am. Chem. Soc.* **2000**, *122*, 7202. (g) Bales, B. L.; Ranganathan, R.; Griffiths, P. C. *J. Phys. Chem. B* **2001**, *105*, 7465.

Scheme 1



developed. Herein we report the first method that allows the capture of a RM without disrupting the prepolymerized dimensions.^{19–21}

Results and Discussion

Amphiphilic Monomer Design and Synthesis. The RM-forming cross-linkable amphiphile used in this study was synthesized with three design criteria in mind: (1) The amphiphile's geometry was designed to be an inverted cone in which the polar portion serves as the apex and the branched 2-ethylhexyl moieties serve as the hydrophobic base.²² (2) The α -methoxyacrylate affords fast polymerization.²³ (3) A carboxylic acid headgroup facilitates further functionalization. As shown in Scheme 2, RM-forming monomer **1** was synthesized via an efficient four-step synthesis. 2-Ethylhexanol was used as the solvent under Baylis–Hillman conditions to provide acrylate **2**.²⁴ The *tert*-butyl ester was removed with trifluoroacetic acid, and the resulting carboxylic acid was converted to the acyl chloride and reacted with 2,2-bis(hydroxymethyl)propionate. The carboxylic acid headgroup provides a flexible handle for easy incorporation of a variety of functional groups via either an ester or an amide. As an example, diethanol amine was installed using oxalyl chloride to activate the carboxylic acid of **1**, providing an amphiphile with a nonionic headgroup (**3**).

Formation and Characterization of RMs. RMs of monomer **1** were evaluated by ¹H NMR spectroscopy and dynamic light scattering (DLS) (Table 1). Monomer **1** was found to be soluble in toluene (>500 mM). Solutions of **1** in toluene dissolved water up to $W_0 = 12$ ($W_0 = [\text{H}_2\text{O}]/[\text{I}]$), and as expected DLS indicated that the mean radius increased with the addition of water.²⁵

In an effort to better characterize the RMs, the proton chemical shift was measured as a function of water content,²⁶ and, as shown in Table 1, the water in the largest core has a chemical shift similar to that of bulk water (4.8 ppm). Consistent with previous reports, as the water core size decreased, the water's chemical shift moved upfield.^{27,28} The change in chemical shift with decreasing water content indicates a change

in water structure as water–carboxylate interactions become more prevalent than water–water interactions.²⁹

Cross-Linking of the RMs. Photoinitiated cross-linking of the RMs using 2,2'-azobis(isobutyronitrile) (AIBN) as the radical initiator proved very sluggish. A mixture of AIBN/benzophenone, however, provided efficient polymerization and was superior to AIBN or benzophenone alone. The course of polymerization was followed by monitoring the loss of the vinyl proton resonances using ¹H NMR spectroscopy. In <5 min, >90% of the vinyl protons were consumed using the mixed initiator system.

Polymerization was monitored as a function of water content (Table 1). The polymerizations yielded macrogelation (the entire solution gels) at W_0 values >10 and gel precipitation at W_0 values between 5 and 10. At low W_0 values, isotropic solutions remained after cross-linking, indicating that the particle size was small. DLS revealed that these isotropic solutions contained particles with 6.5 and 5.5 nm radii when W_0 was 3 and 1.5, respectively. These values are in contrast to previously reported examples in which the particle size increased >20-fold upon polymerization.²¹ In our system, the particle size doubling is most likely caused by particle agglomeration that occurred during the cross-linking.³⁰ The radius of curvature difference between high- W_0 -value particles and low- W_0 -value particles may govern the agglomeration.³¹ In other words, the topology of **1** is a cone of a certain invariant radius, and, as the RMs increase or decrease in size, the cone packs less efficiently. The difference in packing may influence how quickly agglomerated RMs can fuse and bud.

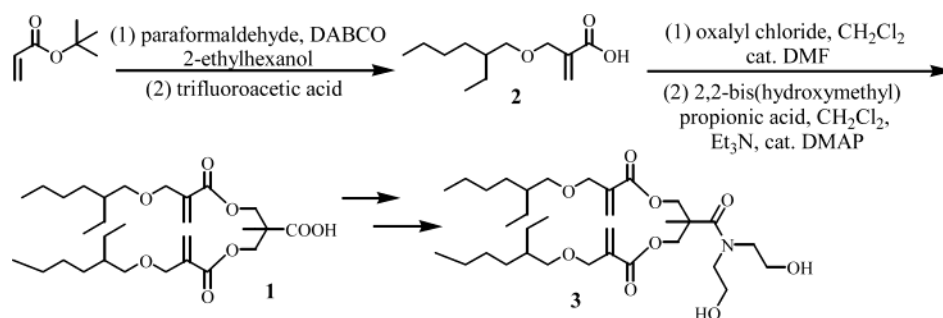
To test the curvature hypothesis, mixed RMs were created, and their response to cross-linking was investigated. The branched nonionic amphiphile **3** was synthesized and was predicted to have a more cylindrical shape than **1**. We predicted that the branching chains should increase the overall headgroup size, thus reducing the pitch. By diluting the anionic carboxylates, the nonionic headgroup also reduces charge–charge repulsion, allowing the amphiphiles to pack more tightly and thereby increasing the average particle diameter. A 9:1 mixture of **1:3** ($W_0 = 2.5$) was made in toluene, the precross-linked radius was 4.5 nm, and the (xRMs) postpolymerization radius was 5 nm. Two features distinguish the **1:3**-RMs from the **1**-RMs: (1) the increase in size upon cross-linking is greatly attenuated, and (2) the precross-linked radii are twice the size of **1**-RMs. The fact that the mixed xRMs do not significantly change upon cross-linking suggests that they are more tightly packed and do not fuse and bud on the same time scale as the **1**-RMs.

Transmission Electron Microscopy (TEM) Images of xRMs. xRMs were prepared using cesium hydroxide as the base to provide an interior coated with heavy atoms. The Cs-xRMs had an average solution radius of 4.9 nm ($W_0 = 1.5$) as determined by DLS, which is larger than the radii found for xRMs with sodium counterions. We found that standard staining methods such as uranyl acetate and phosphomolybdic acid

(19) For a general review of reverse micelles, see: Structure and Reactivity in Inverse Micelles. *Studies in Physics and Theoretical Chemistry* 65; Pileni, M. P., Ed.; Elsevier: New York, 1989.
 (20) For general reviews of polymerizable amphiphiles, see: Miller, S. A.; Ding, J. H.; Gin, D. L. *Curr. Opin. Colloid Interface Sci.* **1999**, *4*, 338.
 (21) (a) Voortmans, G.; Verbeeck, A.; Jackers, C.; De Schryver, F. C. *Macromolecules* **1988**, *21*, 1977. (b) Nagai, K.; Satoh, H.; Kuramoto, N. *Polymer* **1992**, *33*, 5303.
 (22) Israelachvili, J. N. *Intermolecular and Surface Forces*, 2nd ed.; Academic Press: London, 1991.
 (23) Yamada, B.; Kobatake, S.; Aoki, S. *J. Polym. Sci., Part A* **1993**, *31*, 3433.
 (24) Challenger, S.; Derrick, A.; Mason, C. P.; Silk, T. V. *Tetrahedron Lett.* **1999**, *40*, 2187.
 (25) An equivalent of NaOH was combined with the added water to deprotonate the carboxylic acid.
 (26) In a typical preparation, amphiphile **1** was dissolved in deuterated benzene or toluene and H₂O. W_0 was assessed by measuring the ratio of H₂O to amphiphile resonances.
 (27) Li, Q.; Li, T.; Wu, J. *J. Phys. Chem. B* **2000**, *104*, 9011.
 (28) The chemical shift of water in benzene is 0.4 ppm.

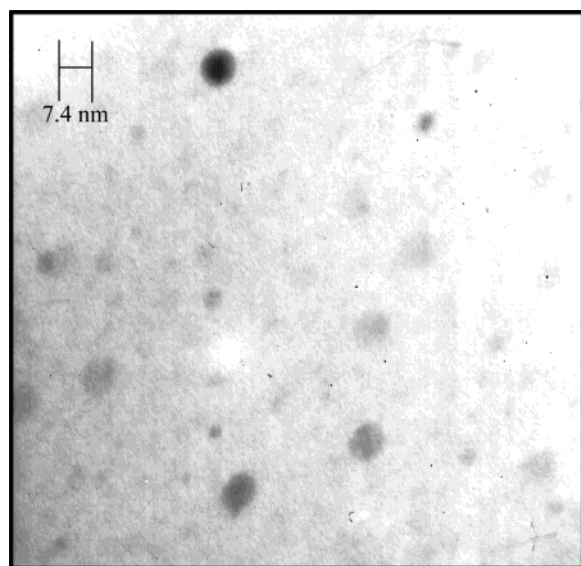
(29) Silber, J. J.; Biasutti, A.; Abuin, E.; Lissi, E. *Adv. Colloid Interface Sci.* **1999**, *82*, 189.
 (30) (a) Lang, J.; Zana, R.; Lalem, N. In *The Structure, Dynamics, and Equilibrium Properties of Colloidal Systems*; Bloor, D. M., Wyn-Jones, E., Eds.; Nato ASI Series Vol. 324; Kluwer: Academic Pub.: Boston, MA, 1989; p 253. (b) Reverse micelles have effectively no monomer/aggregate equilibrium according to: Eicke, H. F. In *Micelles in Aqueous Media*; Mittal, K. N., Ed.; Plenum Press: New York, 1975; Vol. 1, p 429.
 (31) Eastoe, J.; Summers, M.; Heenan, R. K. *Chem. Mater.* **2000**, *12*, 3533.

Scheme 2

**Table 1.** Characterization of RMs Formed with **1** as a Function of W_0

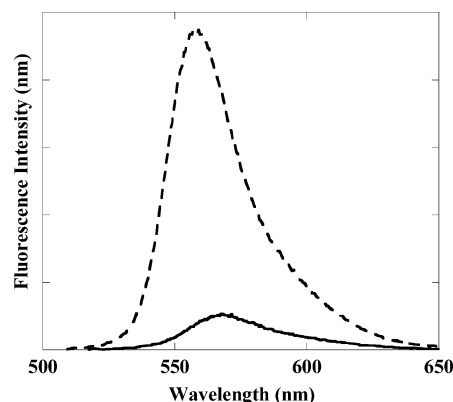
measured W_0^a	^1H of H_2O	DLS (R_h) ^b (nm)	DLS (R_h) ^c (nm)
2.5	4.469	2.03	5.5
4.2	4.588	2.55	6.5
6.0	4.653	2.74	gel ^d
9.9	4.681	3.27	gel ^d
12	4.865	3.47	gel ^d

^a The water content was measured by ^1H NMR spectroscopy by taking the ratio of the water peak to a peak on the amphiphile. The RMs were dissolved in d_6 -benzene. ^b Reverse micelle radius before polymerization. ^c RM radius after polymerization. ^d A gel phase was observed as a precipitate or macrogelation.

**Figure 1.** TEM image of Cs-xRMs on holey carbon grids.

caused the xRMs to aggregate and provided inferior TEM images. As shown in Figure 1, the xRMs are clearly circular, implying that the materials are spherical in solution. Based on the TEM, the average radius was 3.7 nm, which is smaller than the radius found using dynamic light scattering. The TEM images result from electrons scattering off the cesium-lined core and do not reflect the aliphatic chains surrounding the core. A geometry-optimized structure of **1** has a head-to-tail distance of ~ 1.8 nm. The difference between the solution size and the TEM size ($4.9 - 3.7 = 1.2$ nm) is 1.2 nm, indicating that the TEM image is a flattened representation of the spheres or that **1** is not in an extended conformation. Most likely, both are operative.

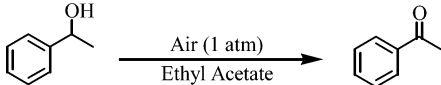
Permeability of xRMs. The permeability of the xRMs was investigated using two different methods. The first method used the water-soluble cationic dye rhodamine 6G (R6G; a toluene-

**Figure 2.** Steady-state fluorescence spectra of R6G excited at 530 nm. The hashed curve (--) is R6G dissolved in a 100 mM NaOAc buffer, and the solid line is R6G within in the xRM core.

insoluble dye) as a marker to investigate whether the xRMs could act as phase-transfer agents. Solutions of R6G in water were extracted with xRMs in toluene. The xRM/toluene solution became brightly colored upon extraction. The fluorescence spectrum of the toluene layer was compared to an aqueous solution of R6G in 100 mM sodium acetate in an effort to mimic the conditions found in an xRM core. The absorption λ_{max} of the R6G/100 mM sodium acetate solution was matched to the xRM/R6G solutions in toluene. Even though both solutions had the same absorbance intensity, the quantum yield of the dye confined within the xRM core was one-sixth that of the dye in aqueous solution (Figure 2). The lower quantum yield results from the self-quenching of the multiple dyes sequestered within each xRM.

We also imbued the xRMs with catalytic function to establish that substrates can enter, react within, and exit the particles. As a model, a *N*-hydroxyphthalimide (NHPI)/cobalt(II) aerobic oxidation was investigated.³² xRMs of **1** ($W_0 = 3$) were used to extract Co(II) ions from an aqueous solution of CoCl_2 . The acetate interior of the particles proved to be an excellent ligand for the Co(II) ions, creating a light blue toluene solution. The light blue cobalt complex in toluene was concentrated to a light purple solid, which was freely soluble in organic solvents and contained 1.83 wt % cobalt as determined by inductively coupled plasma-atomic emission spectroscopy. The ratio of cobalt ions to acetate headgroups is 1:5.8. The UV/vis spectrum of the Co-xRM complex in chloroform shows a broad band between 450 and 700 nm. The λ_{max} was 575 nm with a shoulder at 530 nm. The molar extinction coefficient is $17 \text{ L mol}^{-1} \text{ cm}^{-1}$.

(32) Ishii, Y.; Sakaguchi, S.; Iwahama, T. *Adv. Synth. Catal.* **2001**, *343*, 393. Note: The Co(II)-catalyzed autoxidation at the very least involves the cobalt-mediated oxidation of NHPI to phthalimide *N*-oxyl radical. The cobalt may also directly interact with the *sec*-phenethyl alcohol (see p 409).

Table 2. Turnover Number (TON) and Yield of Acetophenone as a Function of Cobalt Form and Temperature


cobalt form	temp °C	NHPI	TON ^a	conversion ^b
Co-xRM	70	yes	56	100%
Co(OAc) ₂	70	yes	44	88%
Co(Cl) ₂	70	yes	8	47%
Co-xRM	RT	yes	6	17%
Co(OAc) ₂	RT	yes	23	47%
Co(Cl) ₂	RT	yes	2	8%
Co-xRM	70	no	0.5	1%
Co(OAc) ₂	70	no	0.5	1%
xRM	70	yes	2.5	5%
no cobalt	70	yes	2.0	4%

^a Units are in mols of 1-phenylethanol · mols⁻¹ of Co(II) · h⁻¹.

^b Conversion after 4 h of reaction.

From these data, we concluded that the Co(II) species is octahedral and most likely coordinated to water and carboxylates.³³

The Co-xRMs were used to catalyze the autoxidation of *sec*-phenethyl alcohol. Co-xRMs (0.5 mol %) were dissolved in ethyl acetate with NHPI (10 mol %) and *sec*-phenethyl alcohol (100 mM) and stirred at various temperatures under ambient oxygen pressures (see Table 2). At 70 °C, the Co-xRMs catalyze the autoxidation with higher efficiency than does the Co(OAc)₂. Conversely, at room temperature, the Co-xRM efficiency is lower than that of the Co(OAc)₂. The dramatic difference in temperature dependence between the Co-xRMs and Co(OAc)₂ is most likely due to xRM swelling at high temperatures and contraction at lower temperatures.

We systematically investigated the reaction by sequentially leaving out one reaction component. The reaction was extremely slow unless both Co(II) and NHPI were present. The system was compared to Co(OAc)₂ and CoCl₂. Co(OAc)₂ is initially insoluble in ethyl acetate but dissolved under the reaction conditions. The CoCl₂ was insoluble over the entire reaction. These two controls allowed us to probe how our system compares to a soluble and insoluble cobalt catalyst. Our Co-xRM particles catalyze the oxidation significantly better than does insoluble CoCl₂ (see Table 2 for turnover numbers), which is an excellent illustration of the benefits of a freely soluble catalytic domain.

Conclusions

We have synthesized a RM-forming amphiphile and explored its polymerization as a function of water content. At high water content, gel phases were observed, and at low water content, nanometer-size particles were formed. To our knowledge, this report is the first example of RMs being captured as cross-linked spheres whose radii are similar to those of precross-linked RMs. The xRMs can also be created using mixed amphiphile systems, and these mixed systems show a predictably different behavior than do the homo-amphiphile systems.

We also demonstrated that these particles are permeable and that the carboxylate counterions could be exchanged with both fluorescent dyes and transition metal ions, and that the xRMs could act as nanocatalysts in which molecules can enter the

water core, undergo a chemical transformation, and exit. These nanoparticles are currently being functionalized to imbue the spheres with selectivity.

Experimental Methods

General Procedures. Materials were obtained from Aldrich and Acros and were used without further purification. Solvents were purified according to standard procedures. The UV spectra were obtained on a Varian CARY 50 Bio UV/vis spectrophotometer. The ¹H and ¹³C NMR spectra were obtained with a Varian Inova 400 NMR spectrometer. Chemical shifts are reported in δ units using TMS as an internal reference for ¹H NMR and the solvent signal as the reference for ¹³C NMR. The FTIR spectra were recorded on a Mattson Model RS-10500 spectrometer. The DLS measurements were performed using a Proteinsolutions Dynapro 99, and the elemental analysis and ICP analysis were performed by Robertson Microlit Laboratories, Inc. The TEM was carried out on the JEOL-1200 EX in the Cornell Center for Materials Research Electron and Optical Microscopy Facility.

Preparation of *tert*-Butyl 2-(2-Ethylhexyloxymethyl)acrylate. *tert*-Butyl acrylate (10.3 mL, 70 mmol), paraformaldehyde (3.15 g, 110 mmol), and 1,4-diazabicyclo[2.2.2]octane (15.7 g, 14 mmol) were heated at 100 °C in 60 mL of 2-ethylhexanol for 4 days. After being cooled to room temperature, the 2-ethylhexanol was removed under reduced pressure (100 mTorr) at 75 °C, and the remaining residue was purified on a silica gel column (1:1 hexane:ethyl ether) to give 14.6 g (77%) of product as a colorless oil. IR (cm⁻¹, NaCl): 2960 (s), 2930 (s), 2861 (s), 1711 (s), 1642 (m), 1460 (m), 1391 (s). ¹H NMR (400 MHz, CDCl₃): δ 0.86–0.91 (m, 6H), 1.495 (s, 9H), 1.27–1.52 (m, 9H), 3.36 (d, *J* = 5.6 Hz, 2H), 4.12 (s, 2H), 5.78 (d, *J* = 2.0 Hz, 1H), 6.18 (d, *J* = 1.6 Hz, 1H). ¹³C NMR (100 MHz, CDCl₃): δ 12.14, 15.14, 24.12, 24.94, 29.08, 30.17, 31.66, 40.79, 70.24, 74.79, 81.7, 125.1, 140.2, 166.3. Anal. Calcd for C₁₆H₃₀O₃: C, 71.07; H, 11.18. Found: C, 70.98; H, 11.21.

Preparation of 2-(2-Ethylhexyloxymethyl)acrylic Acid (2). A solution of *tert*-butyl 2-(2-ethylhexyloxymethyl)acrylate (14.6 g, 54.0 mmol) in dichloromethane (80 mL) and trifluoroacetic acid (40 mL) was stirred for 1.5 h at room temperature. After evaporation of solvent, the remaining residue was dissolved in dichloromethane (200 mL) and washed with water (3 × 100 mL). The organic phase was dried (Na₂SO₄) and concentrated, giving 11.2 g (96%) of **2**. The product was used for preparation of **1** without further purification. IR (cm⁻¹, NaCl): 2959 (s), 2930 (s), 2861 (s), 1702 (s), 1637 (m), 1457 (m), 1442 (m), 1306 (m). ¹H NMR (400 MHz, CDCl₃): δ 0.86–0.90 (m, 6H), 1.25–1.41 (m, 8H), 1.55 (m, 1H), 3.39 (d, *J* = 5.6 Hz, 2H), 4.17 (s, 2H), 6.00 (d, *J* = 2.0 Hz, 1H), 6.43 (d, *J* = 1.6 Hz, 1H). ¹³C NMR (100 MHz, CDCl₃): δ 12.12, 15.14, 24.12, 24.91, 30.13, 31.60, 40.69, 69.73, 74.94, 128.9, 138.0, 172.4.

Preparation of the Acid-Terminated Amphiphile (1). Oxalyl chloride (1.6 mL, 18.6 mmol) was added to a solution of **2** (1.058 g, 4.6 mmol) in dichloromethane (75 mL) and *N,N*-dimethylformamide (three drops) at 0 °C. After being stirred for 30 min at 0 °C, the reaction was allowed to proceed at room temperature for 2.5 h. [Toluene (10 mL) was added to the reaction mixture and vacuum distilled.] The remaining residue was dissolved in dichloromethane (75 mL), cooled to 0 °C, and then 2,2-bis(hydroxymethyl)propionic acid (0.310 g, 2.3 mmol), 4-(dimethylamino)pyridine (0.066 g, 0.5 mmol), and triethylamine (2.0 mL, 14.3 mmol) were added. After being stirred for 30 min at 0 °C, the reaction was allowed to proceed at room temperature for 14 h. A 1 N aqueous HCl solution (150 mL) was added to quench the reaction mixture. The organic phase was washed with 1 N HCl solution (2 × 100 mL) and brine (2 × 100 mL). It was dried (Na₂SO₄) and then the remaining residue was purified on a silica gel column (gradient: 5:1 hexanes:ether–1:1 hexanes:ether) to give 0.461 g (38%) of **1** as a colorless oil. IR (cm⁻¹, NaCl): 2959 (s), 2930 (s), 2872 (s), 1724 (s), 1639 (m), 1464 (m), 1379 (s). ¹H NMR (400 MHz, CDCl₃): δ 0.85–0.90 (m, 12H), 1.24–1.39 (m, 19H), 1.53 (m, 2H), 3.36 (d, *J*

(33) Cotton, F. A.; Wilkinson, G. *Advanced Inorganic Chemistry*, 5th ed.; Wiley-Interscience: New York, 1988; p 729.

= 5.2 Hz, 4H), 4.14 (s, 4H), 4.36 (s, 4H), 5.90 (d, $J = 1.6$ Hz, 2H), 6.27 (d, $J = 1.6$ Hz, 2H). ^{13}C NMR (100 MHz, CDCl_3): δ 12.12, 15.15, 18.81, 24.12, 24.90, 30.14, 31.60, 40.71, 47.38, 69.91, 74.97, 127.2, 138.0, 166.2, 179.4. Anal. Calcd for $\text{C}_{29}\text{H}_{50}\text{O}_8$: C, 66.13; H, 9.57. Found: C, 65.96; H, 9.72.

Preparation of the Diol-Terminated Amphiphile (3). Oxalyl chloride (1.35 mL, 15.2 mmol) was added to a solution of **1** (2.00 g, 3.8 mmol) in dichloromethane (75 mL) and *N,N*-dimethylformamide (three drops) at 0 °C. The reaction mixture was stirred for 1 h and then allowed to warm to room temperature. After 1 h, the solution was diluted with toluene and distilled. The residue was dissolved in dichloromethane (75 mL) and cooled to 0 °C. Diethanolamine (1.09 mL, 11.4 mmol), 4-(dimethylamino)pyridine (49 mg, 0.4 mmol), and triethylamine (2.1 mL, 15.2 mmol) were added to the solution. The solution was stirred at 0 °C for 30 min and then allowed to proceed at room temperature overnight. The reaction mixture was diluted with dichloromethane and washed with 1 N HCl and aqueous NaHCO_3 . The organic phase was dried (Na_2SO_4) and concentrated under reduced pressure. The crude residue was then purified on a silica gel column (10:1 ethyl acetate:methanol), yielding 615 mg (26%) of **3** as a colorless oil. IR (cm^{-1} , NaCl): 3806 (b), 2943 (d), 2859 (s), 1737 (s), 1647 (s), 1468 (s), 1373 (s). ^1H NMR (400 MHz, CDCl_3): δ 0.87–0.91 (m, 12H), 1.25–1.54 (m, 21H), 2.84 (t, $J = 5.2$ Hz, 2H), 2.94 (t, $J = 5.2$ Hz, 2H), 3.36 (d, $J = 6.0$ Hz, 4H), 3.67 (t, $J = 5.2$ Hz, 2H), 4.13 (s, 4H), 4.29 (t, $J = 5.2$ Hz, 2H), 4.34 (d, $J = 11.2$ Hz, 2H), 4.37 (d, $J = 10.8$ Hz, 2H), 5.91 (d, $J = 1.6$ Hz, 2H), 6.27 (d, $J = 1.2$ Hz, 2H). ^{13}C NMR (75 MHz, CDCl_3): δ 11.16, 14.20, 17.95, 23.16, 23.95, 29.17, 30.65, 39.77, 46.84, 50.78, 60.29, 64.16, 65.68, 68.98, 74.04, 126.4, 137.1, 165.4, 172.6. Anal. Calcd for $\text{C}_{33}\text{H}_{59}\text{NO}_9$: C, 64.57; H, 9.69; N, 2.28. Found: C, 64.50; H, 9.97; N, 2.23.

Preparation of RMs. Compound **1** ($[\mathbf{1}] = 10$ mM) was dissolved in toluene, and water (containing 1 equiv of NaOH to **1**) was added to reach the appropriate water content, W_0 ($W_0 = [\text{water}]/[\text{amphiphile}]$). The solution was hand shaken and sonicated at room temperature for 1 min, and an optically clear solution was obtained. The samples for the DLS were prepared by filtration through a 450 nm size PTFE syringe filter. The water contents of reverse micelles were determined by ^1H NMR in d_6 -benzene. The mixed micelles were made by the same procedure. The water added has 1 equiv of NaOH to total amphiphile concentration (includes both headgroups).

Polymerization of RMs. The RMs assembled from **1** were photopolymerized at various water contents. AIBN (10 mol %) and benzophenone (10 mol %) were dissolved in the reverse micelle solution,

which was generated by the method described above. The sample tubes were then filled with N_2 . The polymerization was initiated by irradiating the sample with a Hanovia 800 lamp (450 W) with a water-cooling jacket at 26 °C for 1 h. The resulting polymer solution was used for light scattering measurements. The disappearance of monomer **1** was observed with ^1H NMR in d_6 -benzene. IR (cm^{-1} , NaCl): 2957 (s), 2926 (s), 2858 (s), 1729 (s), 1580 (m), 1458 (m), 1377 (m). Anal. Calcd for $(\text{C}_{29}\text{H}_{49}\text{NaO}_8)_n$: C, 63.48; H, 9.00. Found: C, 63.37; H, 8.92.

Preparation of Co(II)-Polymer Particles. $\text{CoCl}_2 \cdot 6\text{H}_2\text{O}$ (0.08 mmol, 19 mg) was added to 20 mL of xRM solution, which was generated from 10 mM monomer **1** in toluene solution by the aforementioned method ($[\text{monomer } \mathbf{1}]:[\text{Co}] = 5:1$). The resulting mixture was sonicated at room temperature for 5 min and heated at 80 °C for 30 min under nitrogen. After being cooled to room temperature, the solution was washed with water (3×10 mL). The resulting pink colored toluene phase was concentrated under vacuum at 70 °C to give a purple solid. UV (toluene): $\lambda_{\text{max}} = 575$ nm ($\epsilon = 17$ $\text{M}^{-1} \text{cm}^{-1}$). IR (cm^{-1} , NaCl): 2957 (s), 2927 (s), 2859 (s), 1730 (s), 1577 (m), 1460 (m), 1377 (m). ICP: Co 1.83 wt %.

Oxidation of *sec*-Phenethyl Alcohol. The Co(II)-polymer particle (1.83 wt % of Co, 16 mg) and *N*-hydroxyphthalimide (0.10 mmol, 16 mg) were added to a solution of *sec*-phenethyl alcohol (1.0 mmol) in ethyl acetate (10 mL). The resulting mixture was heated at 70 °C in the open tube. After 4 h, the ethyl acetate was removed under reduced pressure, and the conversion to acetophenone was determined by ^1H NMR.

Preparation of the TEM Sample. A 20 mM solution of **1** in toluene with $W_0 = 1.5$ (3:1 H_2O :cesium hydroxide) was polymerized according to the standard procedure. A portion of the solution (2.5 mL) was concentrated and diluted in dry diethyl ether to give a 10 mM stock solution. The ether solution was filtered (0.45 μm PTFE), and one drop was placed on a grid (300 mesh, 3-mm holey carbon Cu grid, SPI supplies).

Acknowledgment. We thank Cornell University, the Camille and Henry Dreyfus Foundation, and the 3M Untenured Faculty Grant program for financial support. We thank Professor Ealick for equipment access and the CCMR Electron and Optical Microscopy Facility for the use of their transmission electron microscope.

JA0271983